Nano. Chem. Res., 1(1): 33-39, Winter and Spring 2016
DOI: 10.7508/ncr.2016.01.004

# Photocatalytic application of $TiO_2/SiO_2$-based magnetic nanocomposite ($Fe_3O_4@SiO_2/TiO_2$) for reusing of textile wastewater

L. Enayati Ahangar[a,]*, K. Movassaghi[a], M. Emadi[b] and F. Yaghoobi[a]
[a]*Faculty of Chemistry, University of Isfahan, Isfahan 81746-73441, Iran*
[b]*Department of Chemistry, Marvdasht Branch, Azad Islamic University of Marvdasht, Iran*
*(Received 17 December 2014, Accepted 15 August 2015)*

**ABSTRACT:** In this research we have developed a treatment method for textile wastewater by $TiO_2/SiO_2$-based magnetic nanocomposite. Textile wastewater includes a large variety of dyes and chemicals and needs treatments. This manuscript presents a facile method for removing dyes from the textile wastewater by using $TiO_2/SiO_2$-based nanocomposite ($Fe_3O_4@SiO_2/TiO_2$) under UV irradiation. This magnetic nanocomposite, as photocatalytically active composite, is synthesized via solution method in mild conditions. A large range of cationic, anionic and neutral dyes including: methyl orange, methylene blue, neutral red, bromocresol green and methyl red are used for treatment investigations. Neutral red and bromocresol green have good results in reusing treatment. The high surface area of nanocomposites improve the kinetic of wastewater treatment. In this method, by using the magnetic properties of $Fe_3O_4$ nanoparticles, $TiO_2$-based photocatalyst could be separated and reused for 3 times. The efficiency of this method is respectively 100% and 65% for low concentration (10 ppm) and high concentration (50 ppm) of neutral red and bromocrosol green after 3 h treatment. The efficiency of treatment using the second used nanocomposite was 90% for 10 ppm of the same dyes.

**Keywords:** *$Fe_3O_4@SiO_2/TiO_2$ nanocomposite; Photocatalysis; Textile dyeing wastewater; Neutral red; Bromocresol green*

## INTRODUCTION

The foremost application of nanomaterials is in wastewater and air treatment. Recent growing ecological problems related to air and water pollutions have increased necessitate to new methods for pollution removing [1]. For purification of wastewater, several methods such as reverse osmosis [2], photocatalytic [3], ultrafiltration, photo-Fenton [4], oxidation, ozonation [5,6], biological [7,8] and electrochemical methods [9] were developed. Among of these protocols, treatment based on nanoparticles offer excellent prospects for chemical and biological sensing [10].

The estimated total wastewater discharge from textile plants engaged in wet-finishing is noticeable and needs to be treated through economical cost-effective methods [11]. Biological treatment reduces soluble organics and other contaminants in wastewater which are not removed in primary treatment [12]. The progress of treatment processes is followed by various nanostructures of titan dioxide. $TiO_2$ photocatalyst has attracted much attention for the last decade because of its high efficiency [13-16] and also several advantages including inexpensivity, chemically stability, non-toxicity, photogenerating holes and electrons [17,18]. Based on these properties, $TiO_2$ has a wide application in the degradation of pollutants in wastewater, photovoltaic cells, catalysis, photocatalysis, separation, sensors, optical devices and selective absorption [19-21]. The band gap of $TiO_2$ is slightly more than 3.0 eV which means a very small part in the solar radiation could be suitable for the excitation of electrons from the valence band to the conduction band (the ultraviolet part only) [22]. $TiO_2$ as the photocatalyst has recently attracted great interest for using solar radiation as a light source for water and wastewater treatment [18]. On the other hand, magnetic photocatalyst containing a core of $Fe_3O_4$ and a shell of $TiO_2$ has been developed to avoid photodissolution of iron and to prevent $Fe_3O_4$ from acting as an electron hole recombination

*Corresponding author. E-mail: lalehenayati@gmail.com

center. And using a $SiO_2$ layer between $Fe_3O_4$ and $TiO_2$ improves the photocatalytic properties of the composites [18].

Photocatalytic treatment with $TiO_2$ is an emerging wastewater treatment technology with key advantages counting on the lack of mass transfer limitations, operation at ambient conditions and the feasible use of solar irradiation. Photolysis and photocatalytic treatments were carried out over a suspension of titanium dioxide or zinc oxide under artificial irradiation [22]. Yu *et al.* used $TiO_2$ nanoparticles for selective photocatalytic degradation anionic dyes [23]. Krusic's research group developed a method using $TiO_2$/hydrogel nanocomposite for treatment of some textile azo dyes [1]. Lucas *et al.* used $Fe_3O_4@SiO_2@TiO_2$ photocatalyst in combination with UV irradiation for Reactive Blacks [17]. $TiO_2$ photocatalyst, in anatase phase, was used by Hu's group for decoloration of some dyes such as methylene blue, orange G and rhodamine B [24]. Reyens-Gil's group developed $WO_3$-enhanaced $TiO_2$ nanotube photoanodes for organic and oxidized pollutants [25]. Cyclodextrin- functionalized $Fe_3O_4/TiO_2$ core-shell nanocrystal was used for photocatalytic endocrine-disrupting chemical in water by Vasudevan's group [26].

In this study, we have synthesized and used $TiO_2/SiO_2$-based nanocomposite ($Fe_3O_4@SiO_2/TiO_2$) in presence of UV irradiation for removing some dyes from the textile wastewater. For this research, several cationic, anionic and natural dyes including methyl orange, methylene blue, neutral red, bromocresol green and methyl red were applied. Neutral red and bromocrosol green have good results in reuse treatment. By using magnetic particles, the $TiO_2$ composite could be recovered and used three times for treatments. To the best of our knowledge, the simple synthesized $Fe_3O_4@SiO_2/TiO_2$ nanocomposite ($Fe_3O_4@SiO_2/TiO_2$-NC) is able to remove various dyes and UV-Vis spectroscopy as an easy and accessible method can be used for treatment monitoring. The synthesized $Fe_3O_4@SiO_2/TiO_2$ was characterized using FT-IR, UV-Vis and TEM instruments.

## MATERIAL AND METHODS

### Chemicals

Bromocresol green, methyl orange, methyl red, natural red, methylene blue, hydrochloric acid, iron(II) sulfate hepta-hydrate, iron(III) chloride hexa-hydrate, tetraethylammonium hydroxide ($Et_4NOH$), tetraethoxysilane (TEOS) and sodium hydroxide were purchased from commercial sources (Merck, Fluka or Sigma) and used without further purification. The distilled-deionized water was used in all solution preparation (18 MΩ). The stock solutions of the dyes (50 ppm) were prepared freshly in distillated water

Transmission electron microscopy (TEM) (Phillips-CM10 operating at 100 kV) was used for TEM image. The FTIR spectra of the nanoparticles were obtained by Bruker Vector 33 (Made in Germany) driven by OPUS software version 3.1. UV-Vis spectrophotometer (Cary 1E, Varian) and software version 3.00L182 was used for treatment monitoring. The pHs of the solutions were adjusted and measured with a pH meter 744 (Metrohm, Switzerland)

### Preparation of the $TiO_2$ Coated Magnetic ($Fe_3O_4@SiO_2/TiO_2$-NC)

**Preparation of the $Fe_3O_4$ nanoparticles.** Hydrophilic magnetic-nanoparticles were prepared according to Sun’s method [27]. Briefly, 3 ml of iron(II) sulfate solution (2 M) and 10 ml of an iron(III) chloride solution (1 M) were mixed under vigorous mechanical stirring at room temperature and 15 ml of HCl solution (2 M) was used to dissolve the iron salts. An aliquot of 50 ml of tetraethylammonium hydroxide ($Et_4NOH$) was added to the above solution until the solution reached a *p*H of 13. Immediately a black solution was formed. Figure 1 shows the TEM image of $Fe_3O_4$ nanoparticles. Based on TEM image, the ultrafine particle diameter size of the synthesized $Fe_3O_4$ is about 15-25 nm.

**Preparation of $TiO_2$ coated $Fe_3O_4$.** An inertial layer ($SiO_2$) between $TiO_2$ coating and magnetic material was proposed for better coating of $TiO_2$ layer and to avoid photodissolution of iron. 50 mg of magnetite-nanoparticles was dispersed in 20 ml of deionized water containing (TEOS) under sonication for 20 min [28]. The aggregated magnetic particles were separated and the suspension was transferred to another beaker. The separated $Fe_3O_4@SiO_2$ nanoparticles were washed with water and ethanol. For $TiO_2$ coating purpose $Fe_3O_4@SiO_2$ nanoparticles were dispersed in $TiCl_4$ solution [50 ml ethanol containing 2 ml of TEOS]

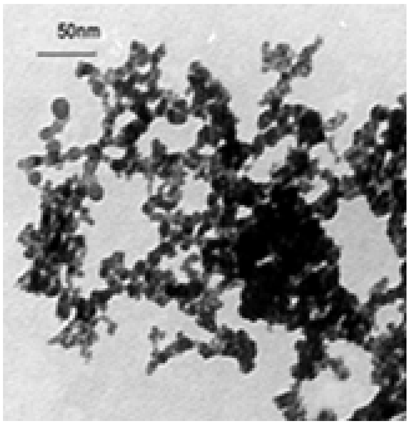


**Fig. 1.**TEM image of $Fe_3O_4$ magnetic nanoparticle.

solution for 30 min under sonication and relaxed for 2 h. After 4 steps washing with ethanol and distillated water, the $Fe_3O_4@SiO_2/TiO_2$ composite was dried and stored [28].

The synthesized nanocomposite was characterized using FT-IR and UV-Vis (Figs. 2a and 2b). The background corrected FT-IR spectra of MNPs are shown in Fig. 2a. The broad band around 3400 $cm^{-1}$ can be assigned to O-H stretching vibration which is assigned to the surface OH groups of $Fe_3O_4$ NPs. The absorption bands around 580-610 $cm^{-1}$ is attributed to the vibration of Fe-O bond in $Fe_3O_4$. In the FT-IR spectrum of $Fe_3O_4@SiO_2$ and $Fe_3O_4@SiO_2/TiO_2$-NC (Figs. 2a and 2b),the band at about 1100 $cm^{-1}$ is assigned to stretch of Si-O bond and the SiO-H/TiO-H groups are appeared by the very broad IR

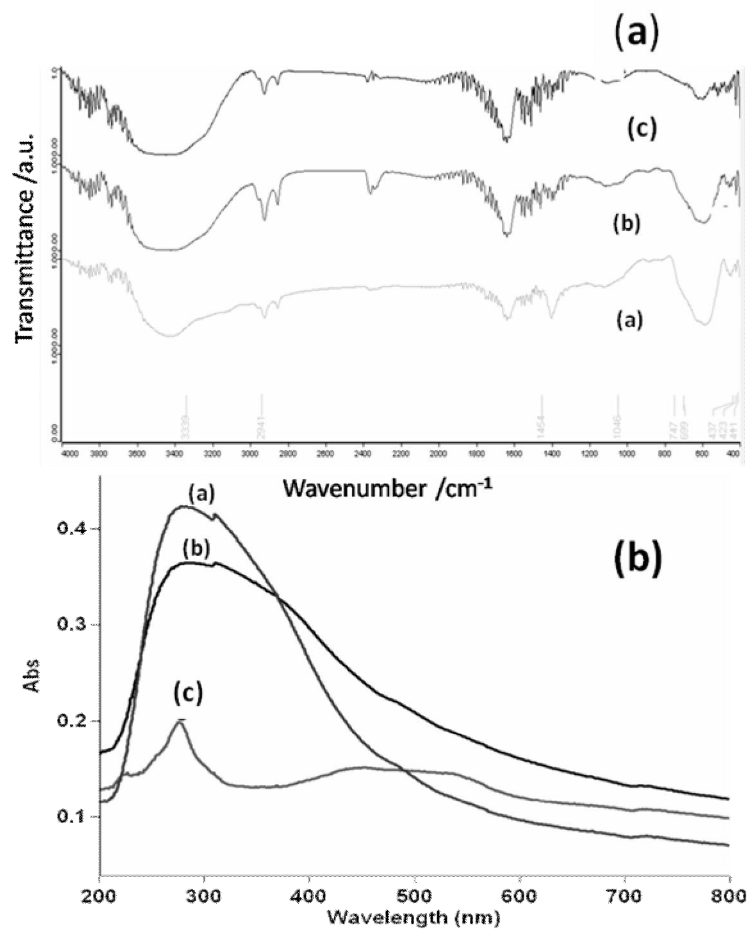


**Fig. 2.** (a) FT-IR and (b) UV-Vis spectra of a: $Fe_3O_4$ nanoparticles, b: $SiO_2$ modified $Fe_3O_4$ nanoparticles and c: $TiO_2$ modified particle.

absorption band in the 2800-3700 $cm^{-1}$ region. In the Fig. 2c, the ratio of 580-610 $cm^{-1}$ to the 1100 $cm^{-1}$ show that the coating of $TiO_2$ is not core-shell nanoparticle. The structure was synthesized as nanocomposite format ($Fe_3O_4@SiO_2/TiO_2$).

For refinement process the $Fe_3O_4@SiO_2/TiO_2$ composite was added to wastewater and mixed by shaker for an appropriate minutes (Table 1), inside of UV irradiation chamber (254 nm) and then test tube was removed from UV chamber and nanocomposite was removed by external magnetic field. Some parameters such as mixing time, amount of $Fe_3O_4@SiO_2/TiO_2$, *p*H and mixing method were optimized. Figure 3 shows the steps of wastewater treatment with $Fe_3O_4@SiO_2/TiO_2$.

## RESULTS

$TiO_2$ photocatalysis is an emerging wastewater treatment technology with key advantages including the lack of mass transfer limitations. Immobilizing $TiO_2$ on $Fe_3O_4$ magnetic nanoparticles is a good strategy enabling the scientists to recover the photocatalysis for several treatment processes [18]. This type of nanoparticle in aqueous solution under UV irradiation is better than that of $Fe_3O_4@TiO_2$ because insulation $SiO_2$ layer prevents photodissolution of Iron. $Fe_3O_4@SiO_2/TiO_2$-NC could be easily separated from wastewater by applying a magnetic field. In this research for achieving a good performance in treatment process several parameters were optimized as will be mentioned in below such as UV irradiation, *p*H, amount of $Fe_3O_4@SiO_2/TiO_2$-NC and treatment time.

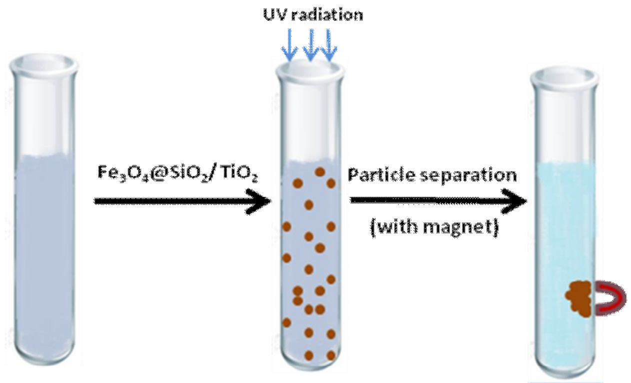


**Fig. 3.** Steps of the proposed wastewater treatment.

## DISCUSSIONS

### Effect of UV Irradiation on Treatment

When solution of dye, neutral red or bromocresol green, was exposed to light in presence of $TiO_2$; initially, the dye molecules, present in singlet ground state, absorb the radiation of suitable wavelength, and are excited to their first excited singlet state. These excited singlet molecules are converted to the triplet excited state [29]. When $TiO_2$

**Table 1.** Comparison Between the Proposed Method and other Reported Techniques for the Photocatalytic treatment method

| Method | Dye | Degradation (%) | Time | Ref. |
|---|---|---|---|---|
| $TiO_2$ nanoparticle | Reactive Brilliant Blue | 100 | 35 min | [23] |
| $TiO_2@SiO_2@Fe_3O_4$ | Reactive Black5 | 91 | 60 min | [17] |
| $TiO_2$/hydrogel nanocomposite | Azo dyes | 75 | 150 min | [1] |
| $TiO_2@Fe_3O_4$ | Pharmaceutical products | 100 | 300 min | [18] |
| $Fe_3O_4@ SiO_2/TiO_2$ | Bromocrosol Green | 100 | 180 min | Present study |

absorbs a photon with equal or greater energy than its band gap width, an electron may be promoted from the valence band to the conduction band leaving behind a hole in the valence band. The electron and hole may migrate to the catalyst surface where they participate in redox reactions with absorbed species. The electron, released from $TiO_2$, will reduce the dye molecule to its colour less products [30]. (Eq. (1)).

$$TiO_2 + h\upsilon \rightarrow e^- + h^+ \qquad (\lambda < 300 \text{ nm}) \qquad (1)$$

For determination the effect of UV irradiation on the degradation process two solutions containing 8 ml of 10 ppm of determined dye and 2 mg of $Fe_3O_4@SiO_2/TiO_2$-NC in different conditions were compared, with and without UV irradiation condition. The Fig. 4 shows the UV-Vis spectrum of these samples. The UV irradiation in $\lambda_{max}$ (254 nm for) improved the treatment up to 65% (decrease percentage of dye absorption) and without UV irradiation no significant treatment was observed.

## Optimization of *p*H and Amount of $Fe_3O_4@SiO_2/TiO_2$-NC

*p*H is an important factor for the interaction of target compounds with mineral oxide surface due to the charge density of nanoparticle which varies strongly with *pH* value. Therefore *p*H is very important in wastewater treatment process with nanomaterial. Also *p*H changes can influence the adsorption of dye molecules onto the $TiO_2$ surfaces, a key step for the photocatalytic oxidation. To obtain a stable colloidal solution of $Fe_3O_4@SiO_2/TiO_2$ a confident amount of acid (HCl) is crucial and this is necessary to preserve the particles in nano-sized structure. The effect of *p*H on the degradation was determined by using different *p*H including 2, 3, 4 and 8. In basic condition especially *p*H 8, there is not any effect and degradation. In acidic condition a good performance for $Fe_3O_4@SiO_2/TiO_2$ was observed. The efficiency of treatment process in different *p*H values is shown in Fig.4. UV-Vis absorption peak at $\lambda_{max}$ 543 nm for acidic *p*H was revealed. The *p*H 3.7 was selected as optimum *p*H for wastewater treatment process (Fig. 5a).

The amount of $Fe_3O_4@SiO_2/TiO_2$-NC can affect the kinetic of the treatment processing. For various amounts of $Fe_3O_4@SiO_2/TiO_2$-NC, the intensity of UV-Vis absorption

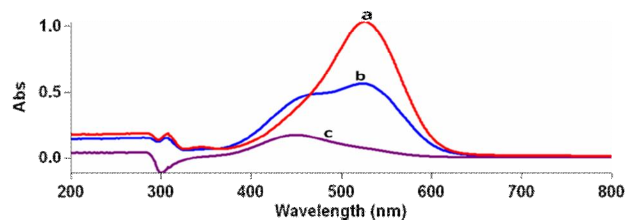


**Fig. 4.** The effect of treatment efficiency of neutral red solution (5 ppm) after 3 h in different conditions, (a) without UV irradiation, (b) with UV and (c) with UV and $Fe_3O_4@SiO_2/TiO_2$ for neutral red.

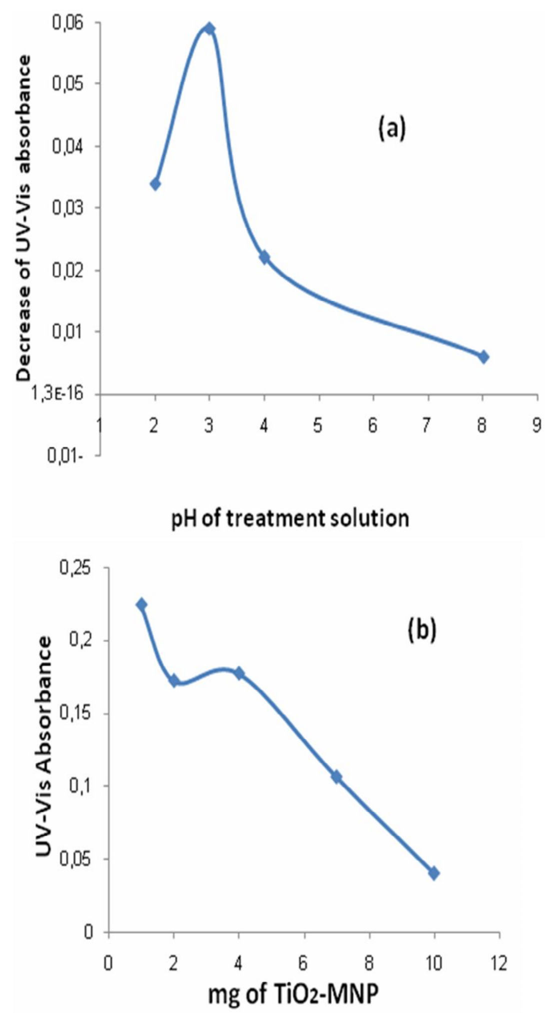


**Fig. 5.** The effect of different (a) pH values and (b) amounts of $Fe_3O_4@SiO_2/TiO_2$ on treatment efficiency.

peak (at wavelength of 543 nm) was monitored for 10 ppm textile color solution (Fig. 5b). In next experiments 2 mg of $Fe_3O_4@SiO_2/TiO_2$-NC, as optimum value, and 8 ml of sample were used for time optimization.

## Optimization of Processing Time

For determination the kinetic of treatment process with $Fe_3O_4@SiO_2/TiO_2$-NC in presence of UV irradiation, different times were checked. For treated wastewater after 3 h, a significant decrease in UV-Vis absorption intensity was observed. UV-Vis absorption intensity of wastewater after different times is shown in Fig. 6. The optimum time was used for next experiments.

## Efficiency of the Proposed Treatment for Different Concentrations

Different concentrations of dyes were used for investigation of treatment efficiency. In Fig. 7 the efficiency of treatment on bromocrosol green is shown. The UV-Vis absorbance of different concentrations of bromocrosol green before and after treatment is shown in Fig. 7. For 2 mg of $Fe_3O_4@SiO_2/TiO_2$-NC, 10 ppm and lower concentration showed excellent efficiency.

## CONCLUSIONS

In this research, efficiency of wastewater treatment for different dyes was determined. Several dyes were used for treatment investigation including methyl orange, ethylene blue, neutral red, bromocrosol green and methyl red. Neutral red and bromocrosol green have shown good results in reusing. In Table 1, Comparison of the proposed methods with other reported techniques is shown. The UV-Vis absorbance of these dyes before and after treatment with $Fe_3O_4@SiO_2/TiO2$-NC and UV irradiation are shown in Fig. 8. $Fe_3O_4@SiO_2/TiO_2$-NC has shown a good efficiency for thetreatment of textile wastewater. The efficiency of this method for neutral red and bromocrosol green is 100% and 65% for low concentration (about 10 ppm) and for high concentration (50 ppm), respectively. Main advantages of this treatment are simplicity and cost-effectiveness. By recovery of used $Fe_3O_4@SiO_2/TiO_2$ and could be at least 3 times. The efficiency of treatment by using the second used nanoparticle was 90% and 50% at low and high

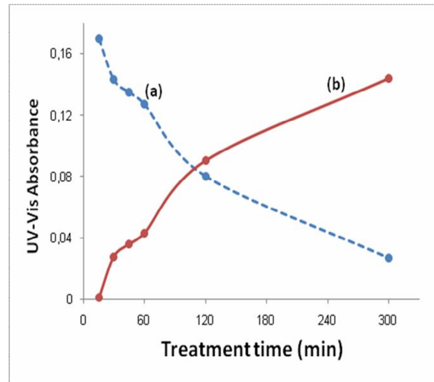


**Fig. 6.** Time optimization for treatment processing (a) UV-Vis absorbance of treated solution, (b) the difference of UV-Vis absorbance between non-treated solution and treated solution for different times.

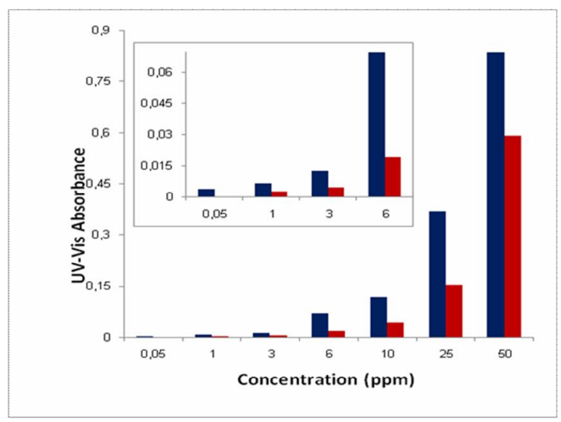


**Fig. 7.** UV-Vis absorbance of wastewater (left) before treatment and (right) after treatment for different concentrations of Bromocresol green.

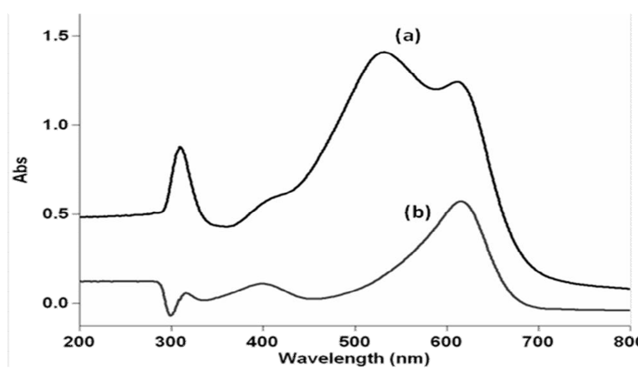


**Fig. 8.** Efficiency of the wastewater treatment for real sample spiked with BCG and bromocrosol green (UV-Vis absorbance a: before and b: after Treatment).

concentrations, respectively. These results show that the complete treatment at high concentration needs to more amount of nanocomposite. Using $Fe_3O_4$@$SiO_2$/$TiO_2$-NC nanocomposite in aqueous solution under UV irradiation is better than $Fe_3O_4$@$TiO_2$because insulation $SiO_2$ layer prevents photodissolution of iron. Efficiency of wastewater treatment for real sample spiked with neutral red and bromocresol green was determined. UV-Vis absorbance of the real wastewater before (curve a) and after treatment (curve b) are shown in Fig. 8.

## ACKNOWLEDGMENTS

The authors would like gratefully acknowledge the financial support of this project by research council of University of Isfahan.

## REFERENCES


[1] M. Lucic, N. Milosavljevic, M. Radetic, Z. Saponjic, M. Rodoicic, M.K. Krusic, 122 (2014) 206.

[2] L.A. Ioannou, C. Michael, N. Vakondios, K. Drosou, N.P. Xekoukoulotakis, E. Diamadopoulos, D. Fatta-Kassinos, Sep. Purif. Technol. 118 (2013) 659.

[3] A.J. Attia, S.H. Kadhim, F.H. Hussein, Eur. J. Chem. 5 (2008) 219.

[4] K. Barbusiński, Pol. J. Environ. Stud. 14 (2005) 281.

[5] M.J. Farre, M.I. Franch, S. Malato, J.A. Ayllon, J. Peral, X. Domenech, Chemosphere 58 (2005) 1127.

[6] H.N. Liu, G.T. Li, J.H. Qu, H.J. Li, J. Hazard. Mater. 144 (2007) 180.

[7] Y.H. Lee, R.D. Matthews, S.G. Pavlostathis, Environ. Res. 78 (2006) 156.

[8] S.P. Buthelezi, A.O. Olaniran, B. Pillay, Molecules 17 (2012) 14260.

[9] D. Dagon, H. Turkdemir, Pol. J. Environ. Stud. 21 (2012) 1185.

[10] V.B. Upadhye, S.S. Joshi, 3 (2012) 264.

[11] Y. Jin, L.Y.L. Yong-kang, L. Jun-ping, Chem. Res. Chinese U. 26 (2010) 278.

[12] J. Perkowski, L. Kos, Fibres Text. East. Eur. 11 (2003) 85.

[13] M. Melemeni, S.D. Stamatakis, N.P. Xekoukoulotakis, Global NEST J. 11 (2009) 357.

[14] W. Zhang, L. Zou, L. Wang, Appl. Catal. A-Gen. 371 (2009) 1.

[15] N.A. Kouamé, D. Robert, V. Keller, N. Keller, C. Pham, P. Nguyen, Environ. Sci. Pollut. R. 19 (2012) 3727.

[16] D. Mahne, U.L. Stangar, P. Trebse, T.G. Bulc, Int. J. Photoenergy 2012 (2012) 1.

[17] M.S. Lucasa, P.B. Tavaresa, J.A. Peresa, J.L. Fariab, M, Rochac, C. Pereirac, Catal. Today 209 (2013) 116.

[18] P.M. Álvareza, J. Jaramilloa, F. López-Pi˜neroa, P.K. Plucinskib, Appl. Catal. B-Environ. 100 (2010) 338.

[19] B. Oregan, M. Gr¨atzel, A Low-cost, Nature 353 (1991) 737.

[20] R. Asahi, T. Morikawa, T. Ohwaki, K. Aoki, Y. Taga, Science 293 (2001) 269.

[21] X. Chen, S.S. Mao, Chem. Rev. 107 (2007) 2891.

[22] F.H. Hussein, T.A. Abass, Int. J. Chem. Sci. 8 (2010) 1353.

[23] Y. Li, W. Zhang, X. Li, Y. Yu, J. Phys. Chem. Solids 75 (2014) 86.

[24] Y. Hsiao, T. Wu, Y. Wang, C. Hu, C. Huang, Appl. Catal. B-Environ. 148-149 (2014) 250.

[25] K.R. Reyes-Gil, D.B. Robinson, ACS Appl. Mater. Interfaces 5 (2013) 12400.

[26] R. Chalasani, S. Vasudevan, ACS Nano 7 (2013) 4093.

[27] J. Sun, S. Zhou, P. Hou, Y. Yang, J. Weng, X. Li, M. Li, J. Biomed. Mater. Res. A 80 (2006) 333.

[28] J.P. Cheng, R. Ma, M. Li, J.S. Wu, F. Liu, X.B. Zhang, Chem. Eng. J. 210 (2012) 80.

[29] O. Sharma, M.K. Sharma, Int. J. Chem. Tech. Res. 5 (2013) 1615.

[30] U.G. Akpan, B.H. Hameed, J. Hazard. Mater. 170 (2009) 520.